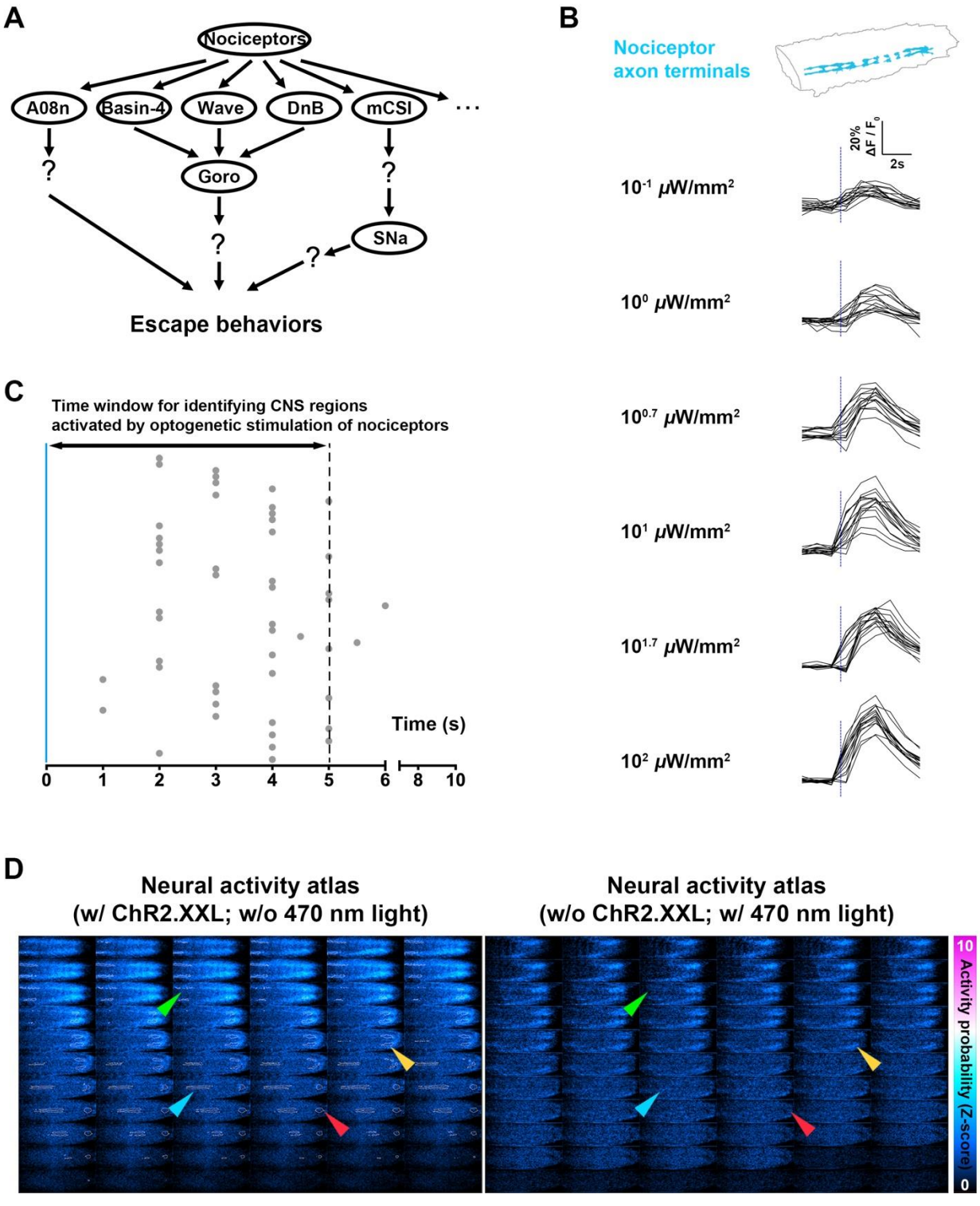

Figure S1. Detailed analysis of functional (calcium) imaging in larval nociceptors and whole-VNC, related to Figure 1 and Figure 2.

(A) Known elements in *Drosophila* larval nociceptive pathway.

(B) Calcium signals ($(F_t-F_0)/F_0$) in larval nociceptor axon terminals upon optogenetic stimulation of nociceptors. Each trace represents the calcium signals in the entire nociceptor axon terminals of a larva. Dotted blue lines represent the optogenetic stimulation onsets.

(C) Define the time window for identifying nociceptor-activated CNS regions in a data-driven manner. Each grey dot represents the median rising time of the first calcium signal after nociceptor stimulation in each whole-VNC activity data. The data is from the experiment shown in Figure 2A. Blue line indicates the timing of optogenetic stimulation of nociceptors. The longest rising time is about 5 sec after nociceptor stimulation (48 out of 50 larvae). Therefore, we define the time window for identifying nociceptor-activated CNS regions as the first 5 sec after stimulation (see STAR Methods for details).

(D) Neural activity atlases without nociceptor activation. Left, no blue light illumination. Right, no ChR2 transgene. Arrows point at nociceptor-activated CNS regions, which are inactive under these conditions. Red, green, yellow, and blue represent PMC, ADs, PDs, and VMs, respectively. N = 30 larvae for the left panel and 20 larvae for right panel.

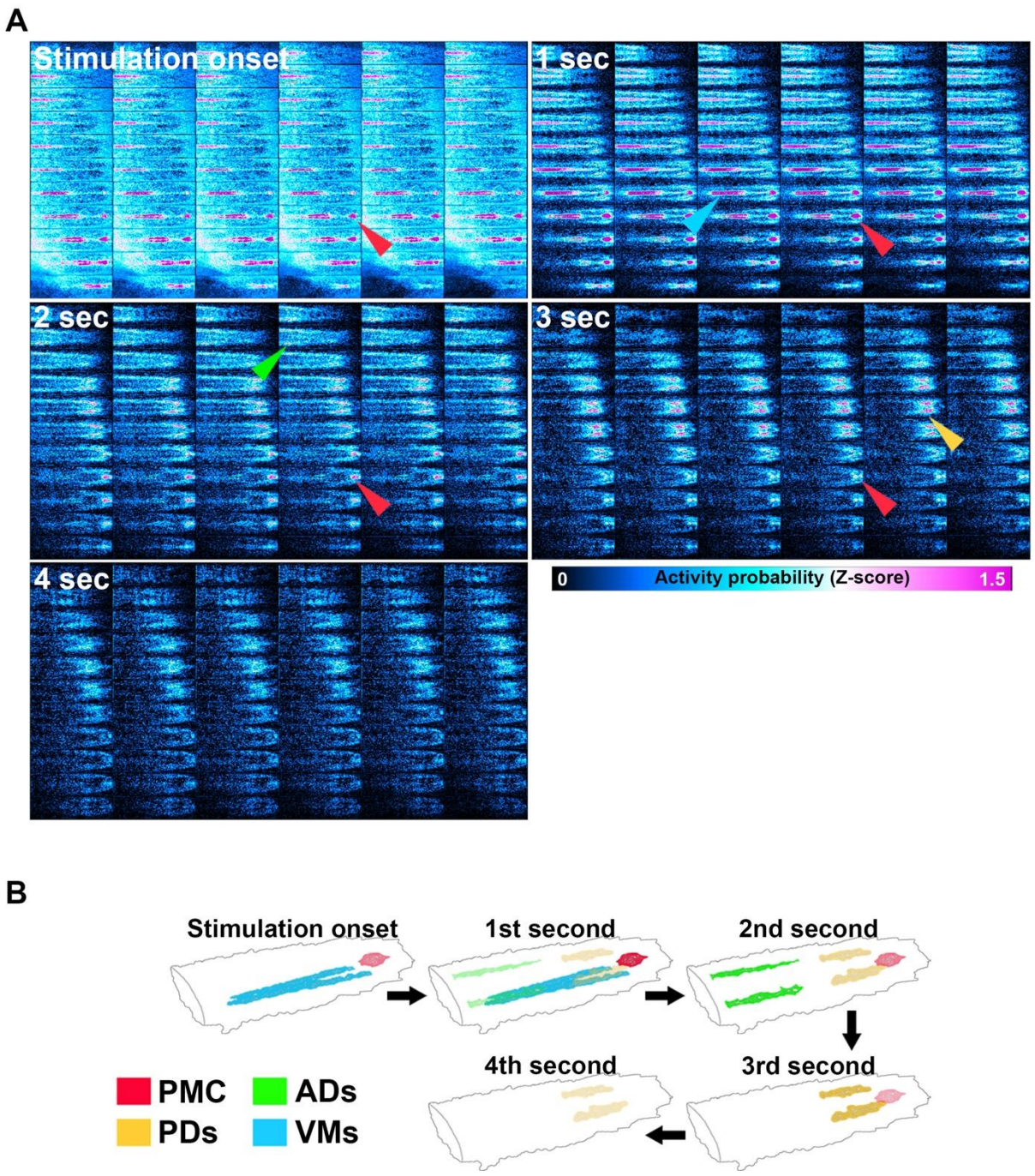

Figure S2. Detailed analysis of whole-VNC functional imaging, related to Figure 2.

(A) Neural activity atlases for each second after nociceptor stimulation, which is the breakdown of neural activity atlas of total 5 seconds upon nociceptor stimulation in Figure 2A. Arrows point at nociceptor-activated CNS regions.

(B) Schemas showing temporal dynamics of nociceptor-activated CNS regions upon nociceptor stimulation (the statistical analysis is shown in Figure 2C).

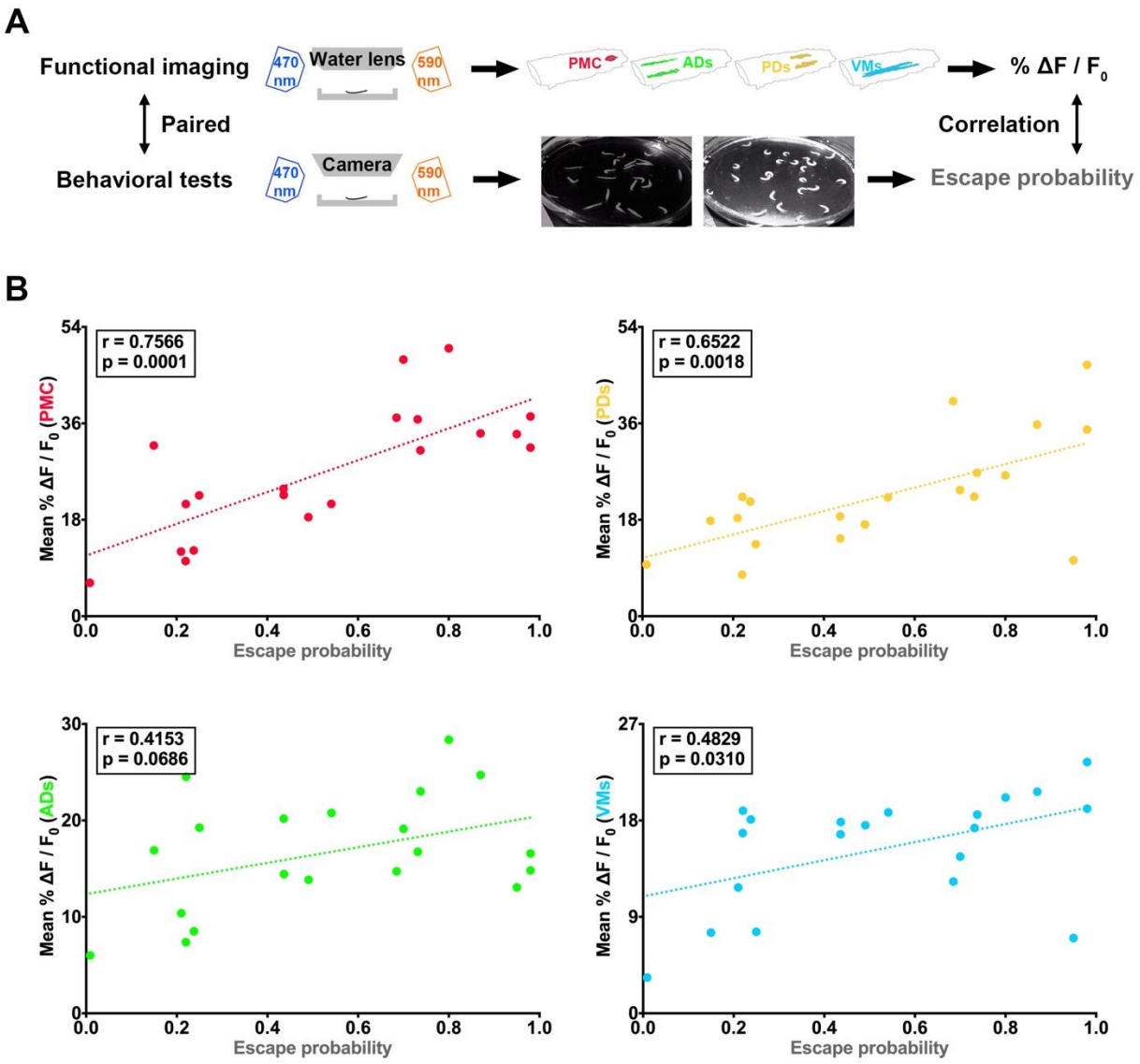

Figure S3. Large-scale of correlation analysis demonstrates that PMC is a decision-associated CNS region, related to Figure 2E.

(A) Schema shows the process of pairing functional imaging and behavioral tests (see STAR Methods for details).

(B) Correlations between escape probability (X-axis) and the activity level of different nociceptor-activated CNS regions (Y-axis) of every experimental group of functional imaging and its paired behavioral data (20 groups, 675 larvae of individual whole-VNC

activity data and 2,294 larvae of paired behavioral data. Each dot represents a group. Pearson correlation coefficients (r). These groups are (from left to right): 0.1 μW/mm^2 in Figures 3A and 3B, 1 μW/mm^2 in Figures 3A and 3B, DnB activation in Figure 2D, A08n inhibition using A08n-split GAL4 (N = 35 larvae for whole-VNC activity data and 100 for paired behavioral data), Basin-4 inhibition in Figures 5D and 5E, A08n inhibition in Figures 5D and 5E, A08n activation in Figure 2D, Wave inhibition in Figures 5D and 5E, mCSI inhibition in Figures 5D and 5E, PDF inhibition in Figure 4A, LK inhibition in Figure 4A, LK activation in Figure 4B, 10 μW/mm^2 in Figures 3A and 3B, DnB inhibition in Figures 5D and 5E, Control group in Figures 5D and 5E, 100 μW/mm^2 in Figures 3A and 3B, Wave activation in Figure 2D, A08n activation using A08n-split GAL4 (N = 20 larvae for whole-VNC activity data and 100 for paired behavioral data), Basin-4 activation in Figure 2D, and mCSI activation in Figure 2D.

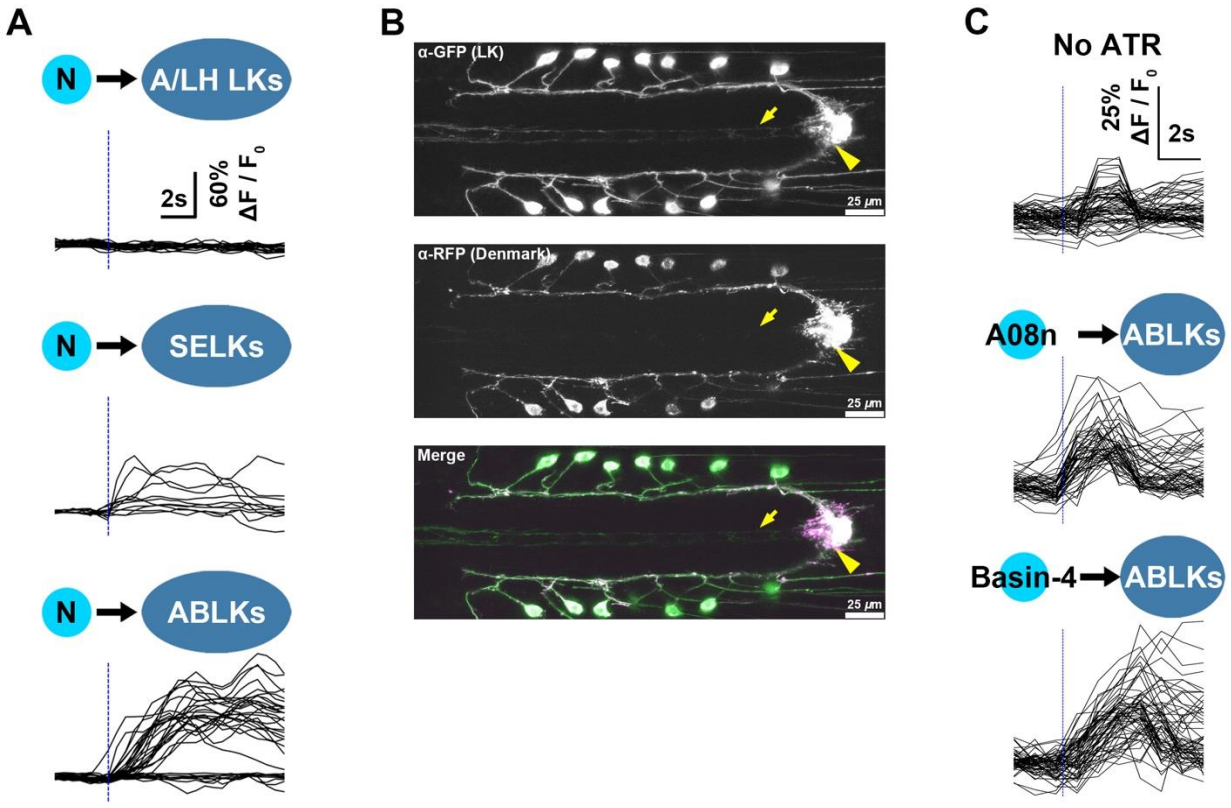

Figure S4. Stimulation of nociceptors or SONs activates ABLK neurons, related to Figure 4.

(A) Nociceptors activate SELKs and ABLKs. N = 3 larvae per group. Each trace represents the calcium signals in a neural structure (3-dimensional region of interest, 3-D ROI), which is an ALK, or LHLK, or SELK or ABLK soma. Dotted blue lines represent the optogenetic stimulation onsets.

(B) Confocal imaging showing LK morphology in the larval VNC (mCD8-GFP). The SELKs send axons to the PMC and ABLKs extend their dendrites (labeled by a dendritic marker, Denmark-mCherry) in the PMC. Arrows point at SELK axons and arrowheads point at ABLK dendrites within the PMC.

(C) SONs activate ABLKs. N = 3, 4 and 5 larvae for light control, A08n and Basin-4, respectively. Each trace represents the calcium signals in an ABLK soma. Dotted blue lines represent the optogenetic stimulation onsets.

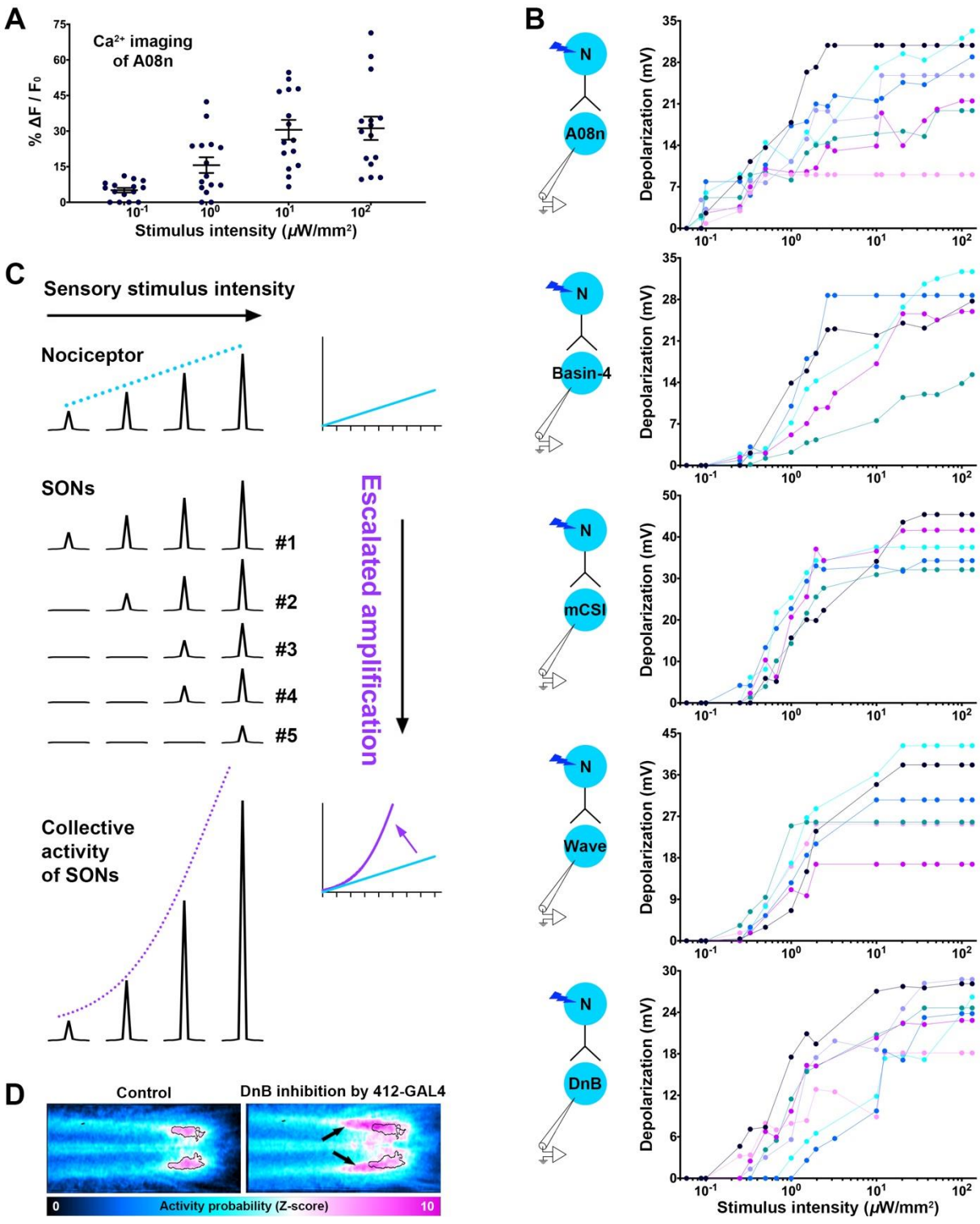

Figure S5. Escalated amplification of nociceptive encodings by SONs, related to Figure 5.

(A) The calcium responses of A08n neurons upon different intensities of nociceptor stimulation. Each dot represents the averaged calcium responses in two A08n neurons of a larva. N = 15 larvae per intensity group.

(B) Electrophysiological recordings (whole-cell path-clamp) of SONs (A08n, Basin-4, mCSI, Wave, DnB) under different intensities of nociceptor stimulation. These data include those in Figures 5A, 5B and 5C. The sample numbers and genotypes are the same as those in Figures 5A, 5B and 5C. Each dot represents the averaged depolarization amplitude from at least 3 individual recordings of the same cell at a stimulus intensity. For each cell, the optogenetic stimulation was performed from low intensity to high intensity in order to identify the minimum and maximum responses of this cell. 3-7 individual cells (different colors indicate different individual cells) were recorded at each stimulation intensity.

(C) A schematic explaining how recruitment of SONs might lead to escalated amplification of graded sensory encodings. The increases of both activated cell number and activity level in each cell result in a quadratic (escalated amplification) increase of the summed responses.

(D) Representative z planes from neural activity atlases for control and DnB inhibition by 412-GAL4 (the same z plane). Black arrows point at hyper-activated regions outside the nociceptor-activated CNS regions. This is because 412-GAL4 also labels large amount of GABAergic inhibitory neurons in the VNC and inhibiting these neurons by GtACR1 causes hyper-activity throughout the VNC. Data is from the experiments shown in Figure 5D.

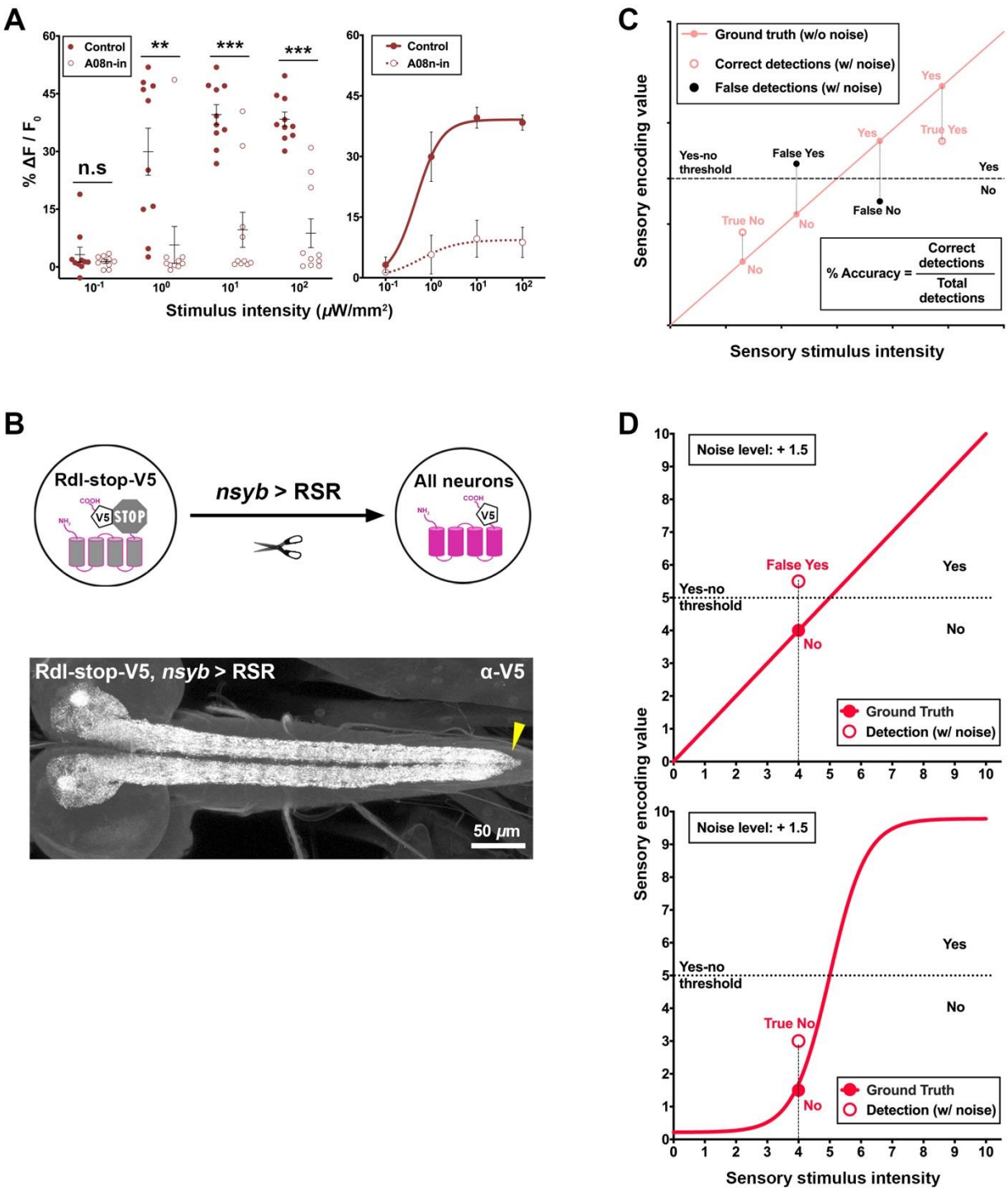

Figure S6. The gated amplification mechanism enhances the accuracy in binary decisions, related to Figure 6 and Figure 7.

(A) Inhibition of A08n neurons results in a less-steep stimulus-response curve of activity level in ABLK neurites within the PMC region. Left: each dot represents a larva. N = 10 per genotype at each intensity for control and A08n-in, respectively. Right: each dot represents the mean activity level of an intensity group. Logistic (sigmoid) fittings are used for both curves.

(B) Confocal imaging showing endogenous *Rdl* (tagged by V5) expression patterns when R-recombinase (RSR) is expressed in all neurons (*nsyb* > RSR). Schemas showing the design and use of *Rdl*-stop-V5 knock in fly. RSR is used to excise isoTarget cassette (translational stop cassette) to enable V5 to tag endogenous *Rdl*. Endogenous *Rdl* is expressed exclusively in neurites (neuropils) but not in somas. Arrowhead points at *Rdl* expressing area in the PMC.

(C) The definitions of parameters in the computational modeling. Detection was defined as a sensory encoding value above the yes-or-no threshold. Accuracy was defined based on the signal detection theory.

(D) A drawing illustrating that the same level of noise is less likely to cause binary (sigmoid) signals than graded (linear) ones to falsely pass the decision threshold.

Figures / abbreviation	Genotype
Figure 1A	*Canton S*
Figures 1C-1E	; LexAop2-jRCaMP1b / +; *TrpA1*-QF, QUAS-ChR2T159C / *ppk*-LexA
Figure 2A	; *nsyb*-LexA, LexAop2-jRCaMP1b / +; *ppk*-ChR2.XXL, UAS-GtACR1 / +
Figure 2D / A08n	; *nsyb*-LexA, LexAop2-jRCaMP1b / UAS-ChR2.XXL; 82E12-GAL4 / +
Figure 2D / Basin-4	; *nsyb*-LexA, LexAop2-jRCaMP1b / UAS-ChR2.XXL; 57F07-GAL4 / +
Figure 2D / mCSI	; *nsyb*-LexA, LexAop2-jRCaMP1b / UAS-ChR2.XXL; 94B10-GAL4 / +
Figure 2D / Wave	; *nsyb*-LexA, LexAop2-jRCaMP1b / UAS-ChR2.XXL, MB120B-GAL4.AD; MB120B-GAL4.DBD / +
Figure 2D / DnB	; *nsyb*-LexA, LexAop2-jRCaMP1b / UAS-ChR2.XXL; 412-GAL4 / +
Figures 3A-3C	; *nsyb*-LexA, LexAop2-jRCaMP1b / +; *TrpA1*-QF, QUAS-ChR2T159C / +
Figure 4A / Control	; *nsyb*-LexA, LexAop2-jRCaMP1b / +; *ppk*-ChR2.XXL, UAS-GtACR1 / +
Figure 4A / LK	; *nsyb*-LexA, LexAop2-jRCaMP1b / LK-GAL4; *ppk*-ChR2.XXL, UAS-GtACR1 / +
Figure 4A / PDF	PDF-GAL4 / +; *nsyb*-LexA, LexAop2-jRCaMP1b / +; *ppk*-ChR2.XXL, UAS-GtACR1 / +
Figure 4A / Mip	; *nsyb*-LexA, LexAop2-jRCaMP1b / +; *ppk*-ChR2.XXL, UAS-GtACR1 / Mip-GAL4
Figure 4A / DSK	; *nsyb*-LexA, LexAop2-jRCaMP1b / +; *ppk*-ChR2.XXL, UAS-GtACR1 / DSK-GAL4
Figure 4A / CCAP	; *nsyb*-LexA, LexAop2-jRCaMP1b / CCAP-GAL4; *ppk*-ChR2.XXL, UAS-GtACR1 / +
Figure 4A / FMRFa	; *nsyb*-LexA, LexAop2-jRCaMP1b / +; *ppk*-ChR2.XXL, UAS-GtACR1 / 61H09-GAL4
Figure 4A / NPF	; *nsyb*-LexA, LexAop2-jRCaMP1b / +; *ppk*-ChR2.XXL, UAS-GtACR1 / NPF-GAL4
Figure 4B / No GAL4	; *nsyb*-LexA, LexAop2-jRCaMP1b / UAS-ChR2.XXL;
Figure 4B / LK	; *nsyb*-LexA, LexAop2-jRCaMP1b / LK-GAL4, UAS-ChR2.XXL;
Figure 4B / PDF	PDF-GAL4 / +; *nsyb*-LexA, LexAop2-jRCaMP1b / UAS-ChR2.XXL;
Figure 4C	; LK-GAL4 / +; UAS-jRCaMP1b, *TrpA1*-QF, QUAS-ChR2T159C / +;
Figure 4D / LK inhibition	; LK-GAL4 / nsyb-LexA, LexAop2-jRCaMP1b; UAS-GtACR1, *TrpA1*-QF, QUAS-ChR2T159C / +;
Figure 4E	; LK-GAL4 / +; UAS-CsChrimson / +
Figures 5A-5C / A08n	; UAS-mCherry / +; *TrpA1*-QF, QUAS-ChR2T159C / 82E12-GAL4
Figures 5A-5C / Basin-4	; UAS-mCherry / +; *TrpA1*-QF, QUAS-ChR2T159C / 57F07-GAL4
Figures 5A-5C / mCSI	; UAS-mCherry / +; *TrpA1*-QF, QUAS-ChR2T159C / 94B10-GAL4
Figures 5A-5C / Wave	; UAS-mCherry / MB120B-GAL4.AD; *TrpA1*-QF, QUAS-ChR2T159C / MB120B-GAL4.DBD
Figures 5A-5C / DnB	; UAS-mCherry / +; *TrpA1*-QF, QUAS-ChR2T159C / 412-GAL4
Figures 5D and 5E / A08n	; *nsyb*-LexA, LexAop2-jRCaMP1b / +; *ppk*-ChR2.XXL, UAS-GtACR1 / 82E12-GAL4
Figures 5D and 5E / Basin-4	; *nsyb*-LexA, LexAop2-jRCaMP1b / +; *ppk*-ChR2.XXL, UAS-GtACR1 / 57F07-GAL4
Figures 5D and 5E / mCSI	; *nsyb*-LexA, LexAop2-jRCaMP1b / +; *ppk*-ChR2.XXL, UAS-GtACR1 / 94B10-GAL4
Figures 5D and 5E / Wave	; *nsyb*-LexA, LexAop2-jRCaMP1b / MB120B-GAL4.AD; *ppk*-ChR2.XXL, UAS-GtACR1 / MB120B-GAL4.DBD
Figures 5D and 5E / DnB	; *nsyb*-LexA, LexAop2-jRCaMP1b / +; *ppk*-ChR2.XXL, UAS-GtACR1 / 412-GAL4
Figure 6A	; LK-GAL4, UAS-mCD8GFP / LK-GAL4; *Rdl*-stop-V5, UAS-RSR / +;
Figures 6B and 6C / Control	LK-GAL4 / +; LK-GAL4 / +; UAS-jRCaMP1b, *TrpA1*-QF, QUAS-ChR2T159C / +;
Figures 6B and 6C / Rdl-IR	LK-GAL4 / +; LK-GAL4 / UAS-*Rdl*-IR; UAS-jRCaMP1b, *TrpA1*-QF, QUAS-ChR2T159C / +;
Figure S1D / no light	; *nsyb*-LexA, LexAop2-jRCaMP1b / +; *ppk*-ChR2.XXL, UAS-GtACR1 / +
Figure S1D / no ChR2	; *nsyb*-LexA, LexAop2-jRCaMP1b / +; UAS-GtACR1 / +
Figure S3 / A08n-in (splitGAL4)	; *nsyb*-LexA, LexAop2-jRCaMP1b / 82E12-GAL4.AD; 6.14.3-GAL4.DBD / *ppk*-ChR2.XXL, UAS-GtACR1
Figure S3 / A08n-at (splitGAL4)	; *nsyb*-LexA, LexAop2-jRCaMP1b / UAS-ChR2.XXL, 82E12-GAL4.AD; 6.14.3-GAL4.DBD / +
Figure S4A	; LK-GAL4 / +; UAS-jRCaMP1b, *ppk*-ChR2.XXL / +
Figure S4B	; LK-GAL4, UAS-mCD8-GFP / +; UAS-DenMark / +
Figure S4C / light control	; LK-GAL4 / +; LexAop2-ChR2T159C / UAS-jRCaMP1b
Figure S4C / A08n	; LK-GAL4 / 82E12-LexA; LexAop2-ChR2T159C / UAS-jRCaMP1b
Figure S4C / Basin-4	; LK-GAL4 / 57F07-LexA; LexAop2-ChR2T159C / UAS-jRCaMP1b
Figure S5A	; LexAop2-jRCaMP1b / 82E12-LexA; *TrpA1*-QF, QUAS-ChR2T159C / +
Figure S6A / Control	LK-GAL4 / +; LexAop2-GtACR1 / +; *TrpA1*-QF, QUAS-ChR2T159C, UAS-jRCaMP1b / +
Figure S6A / A08n-in	LK-GAL4 / +; LexAop2-GtACR1 / 82E12-LexA; *TrpA1*-QF, QUAS-ChR2T159C, UAS-jRCaMP1b / +
Figure S6B	; ; *nsyb*-GAL4 / UAS-RSR, *Rdl*-stop-V5

Table S1. All genotypes in the figures, related to Figures 1-6.